JOURNAL OF SOLID STATE CHEMISTRY **34**, 207–213 (1980)

Ferrimagnetism in the Rare Earth Titanium (III) Oxides, $RTiO_3$; R = Gd, Tb, Dy, Ho, Er, Tm

CARL W. TURNER AND J. E. GREEDAN

Institute for Materials Research and Department of Chemistry, McMaster University, Hamilton, Ontario, L8S 4M1, Canada.

Received June 13, 1979; in revised form August 23, 1979

The series of compounds $RTiO_3$, R = Gd, Tb, Dy, Ho, Er, and Tm, were obtained as single-phase materials via solid state reaction between Ti_2O_3 and R_2O_3 at ca. 1500°C in welded molybdenum crucibles under argon; $YbTiO_3$ and $LuTiO_3$ could not be obtained as single-phase materials using this procedure. Lattice constants for all compounds were determined from powder X-ray data and are compared with previous results. All of these materials order magnetically between 30 and 70 K. From the appearance of the χ_m^{-1} vs T curve the type of order can be identified as ferrimagnetic. High-temperature susceptibility data have been fit to a two-sublattice molecular field model and the intra- and intersublattice interaction constants have been extracted. It is found that the Ti–Ti interaction is ferromagnetic and relatively constant from R = Gd to R = Lu. Low-temperature magnetization field data suggest the existence of complex magnetic structures, large magnetocrystalline anisotropy, or both. The magnetic properties of the $RTiO_3$ series are compared to those of the chemically similar and better-known RMO_3 phases where M = Al, V, Cr, Mn, and Fe. The observed differences are shown to follow from the sign of the M–M interaction, which is ferromagnetic for M = Ti and antiferromagnetic for M = V, Cr, Mn, and Fe, together with the implications of the crystal symmetry for the R–M interaction.

Introduction

Materials of the composition RMO_3 where R is a rare earth and M a trivalent ion such as Al, Ga, V, Cr, Mn, or Fe have been known for more than 20 years. Extensive reviews of their structure and magnetic properties exist (*1–3*). All of the RMO_3 phases crystallize in some form of the perovskite structure, usually the orthorhombic modification, the so-called $GdFeO_3$ structure type, space group *Pbnm* (No. 62). The Magnetic properties of the RMO_3 compounds generally fall into two classes. When M is nonmagnetic, paramagnetic behavior is observed to 4.2 K, long-range order due to the R^{3+} species being found, if at all, only at lower temperatures. When M is a transition metal ion, long-range order is observed with critical temperatures of the order 10^2 K due to antiferromagnetic (AF) order, usually type G, on the M sublattice. Often, weak ferromagnetism due to sublattice canting is evident. For most of these compounds the R and M magnetic sublattices can be treated as nearly independent (*3*), the R sublattice coupling weakly, if at all, to the M sublattice near 4.2 K where the R sublattice orders independently of M. As pointed out by Gilleo (*4*) the near absence of the R–M interaction is a symmetry effect. In the $GdFeO_3$ structure one can identify a pseudocubic subcell (slight monoclinic distortion) in which R is at the body centre of a simple cubic M lattice. If the M sublattice has AF ordering the R ion will see two sets of

0022-4596/80/110207-07$02.00/0

Printed in Great Britain

four M neighbors with antiparallel spin configurations and the net R–M interaction will be negligible.

Except for an early report that $GdTiO_3$ was ferromagnetic (*5*), compounds from the series $RTiO_3$ had not been studied until recently (*6–10*). The scant evidence available suggested that the magnetic properties of this group might be rather different from those of the other RMO_3 phases. For example, $YTiO_3$ is a ferromagnet (*6, 9, 10*)). As the ionic radius of Y^{3+} is similar to that of Ho^{3+} it was suspected that the Ti–Ti interaction for at least the second half of the $RTiO_3$ series, R = Gd to Lu, might also be ferromagnetic. In such a case R–Ti interactions would not be subject to cancellation by symmetry and the magnetic properties of these materials might be rather different from those of the related RMO_3 compounds.

These expectations have proved to be well founded and we report here the bulk magnetic and structural properties for $RTiO_3$, R = Gd, Tb, Dy, Ho, Er, and Tm. Limited data are also available for $YbTiO_3$ and $LuTiO_3$. These materials form a related subgroup within the $RTiO_3$ series, the common feature being ferrimagnetism. Those phases for which R = La, Ce, Pr, Nd, and Sm exhibit quite different magnetic properties which will be the subject of a subsequent publication.

Experimental

Sample Preparation

The general procedure was to fire well-mixed equimolar amounts of R_2O_3 and Ti_2O_3 sealed in molybdenum crucibles under argon at 1500 to 1800°C for 12 hr. In this manner single-phase products were obtained in all cases except $YbTiO_3$ and $LuTiO_3$. In these two cases lines from a cubic impurity phase comprising perhaps 10% of the sample were always detected in the X-ray powder pattern. For several attempted preparations of $LuTiO_3$, the cubic impurity phase could be identified as Lu_2O_3. This casts some doubt on the stoichiometry of the perovskite phase found in this preparation but for want of more precise information we will refer to that phase as $LuTiO_3$. The impurity lines found in $YbTiO_3$ preparations did not correspond to any previously known phase. For the case of the $LuTiO_3$ preparations small, black, tabular crystals were found on the pellet surfaces. These proved to be crystals of the perovskite phase by precession photography and about 30 mg were isolated. This was a sufficient quantity for determination of a critical temperature and some other magnetic properties but not for chemical analysis. The R_2O_3 (99.99% relative to other rare earths) were used as obtained from Research Chemicals except for a prefiring in air at 1000°C. Tb_2O_3 was prepared from Tb_4O_7, same purity and supplier, by H_2 reduction at 1350°C for 8 hr. Ti_2O_3 was prepared from Ti sponge (99.99%) and TiO_2 (99.95%) by arc melting in a purified Ar/He atmosphere. Stoichiometry was controlled to an $O/Ti = 1.500 \pm 0.005$ and was monitored by thermal gravimetric analysis (tga).

Sample Characterization and Analysis

Phase purity was determined by X-ray powder diffraction using a Philips diffractometer and Cu$K\alpha$ radiation. Precision lattice constants were determined on the same diffractometer using an internal standard of polycrystalline Si, 99.999%, $a_0 = 5.4301$ Å, and at least 15 unambiguously indexed reflections.

Chemical analysis of these materials is difficult. It has thus far proved impossible to dissolve them using any standard technique including bisulfite fusions and high-pressure (30 atm), high-temperature (240°C) treatment with HF/H_2SO_4. Ti^{3+} content can be determined by tga in air assuming oxidation to Ti^{4+} and the R/Ti ratio can be determined in favorable cases by neutron activation analysis on powders.

Magnetic Measurements

Magnetic data were collected using a PAR vibrating sample magnetometer between 4.2 and 300 K. Temperature was measured using a calibrated iron-gold thermocouple. The magnetometer was calibrated with a sample of high-purity nickel. Magnetic fields in the range of 6.0 T were obtained from a superconducting solenoid.

Results and Discussion

Chemical Analysis

The results of the tga and neutron activation analyses are presented in Table I.

The materials prepared and used in this study are not grossly nonstoichiometric within the limits of our analytical methods. As the YbTiO_3 and LuTiO_3 phases could not be prepared as single phases, their analytical data are not included in the table.

Crystal Chemistry

All lines in the powder patterns of all of the phases studied here, except YbTiO_3 and LuTiO_3, could be indexed on an orthorhombic cell of the type appropriate to *Pbnm* symmetry. Lines belonging to a similar orthorhombic cell could be assigned from the two-phase powder patterns of YbTiO_3 and LuTiO_3. Single-crystal data (*11*) for GdTiO_3 and YTiO_3 (the ionic radii of Y^{3+} and Ho^{3+} are essentially equal) (*12*) establish the *Pbnm* space group for these two materials and, by reasonable extension, for the remaining members of this series. Cell constants and cell volumes are given in Table II and a plot of cell volume versus the cube or the R^{3+} radius is presented in Fig. 1. The values in Table II differ slightly from those quoted in a preliminary report (*8*) due to reindexing of some diffraction lines. The cell volume varies in a linear manner with the R^{3+} ionic volume. Our values are in reasonable agreement with those reported previously by McCarthy *et al.* (*13*).

TABLE I

ANALYTICAL DATA FOR $R\text{TiO}_3$ PHASES

Percentage weight gain by oxidation				
R	Exp.	Theor.	Diff.	R/Ti neutron activation
Gd	3.11	3.16	−1.58	—
Tb	3.13	3.14	−0.32	—
Dy	2.99	3.10	−3.55	—
Ho	3.06	3.07	−0.33	1.02 ± 0.01
Er	2.99	3.04	−1.64	0.998 ± 0.010
Tm	3.09	3.02	+2.32	—

Magnetic Properties

Figures 2a and b display the temperature dependence of the inverse magnetic susceptibility for the materials studied here. Note that Curie–Weiss behavior is found from 300 to about 120 K, below which negative deviations set in. In fact, these curves have the familiar hyperbolic shape characteristic of two-sublattice ferrimagnets. This is the first evidence that the intersublattice interaction is relatively more important in the $R\text{TiO}_3$ compounds than in the corresponding $R\text{CrO}_3$ and $R\text{FeO}_3$ phases. We have fit our susceptibility data to the appropriate function (*13*),

$$\chi_{\mathrm{m}}^{-1} = \frac{T-\theta}{C} - \frac{\xi}{T-\theta'},$$

TABLE II

UNIT-CELL DATA FOR VARIOUS $R\text{TiO}_3$

R	a (Å)	b (Å)	c (Å)	Volume (Å^3)
Gd[a]	5.393(2)	5.691(2)	7.664(3)	235.2
Tb	5.355(2)	5.665(2)	7.647(4)	232.0
Dy	5.355(2)	5.681(2)	7.655(3)	232.9
Ho	5.347(2)	5.672(5)	7.621(5)	230.9
Er	5.295(2)	5.649(2)	7.588(2)	226.9
Tm	5.293(2)	5.648(2)	7.586(3)	226.8
Yb	5.288(3)	5.638(3)	7.585(4)	226.1
Lu	5.282(2)	5.617(1)	7.585(3)	225.0

[a] Data from a single crystal; all other data are from powders. The numbers in parentheses are the standard deviations in the last significant figure.

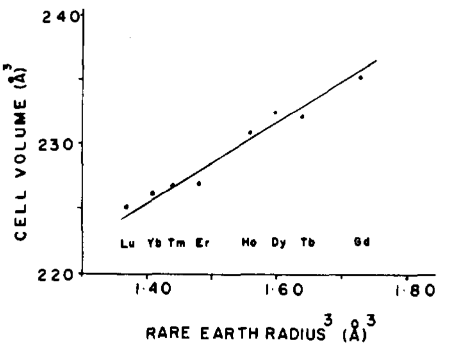

FIG. 1. Correlation between unit-cell volume and the cube of the R^{3+} radius for various $R\mathrm{TiO}_3$. The radii are those for VIII-fold coordination (*12*).

based on the molecular field model for the two-sublattice ferrimagnet and the parameters are given in Table III. Also in Table III we report the molecular field coupling constants $\gamma_{\mathrm{Ti-Ti}}$, $\gamma_{\mathrm{R-Ti}}$, and γ_{R-R} derived from these fitting parameters.

A number of the entries in Table III require comment. As the constant, *C*, is determined from the Curie–Weiss part of the curve its value should be equal to $C_{R^{3+}} + C_{\mathrm{Ti}^{3+}}$ (0.37) and this number is listed in the column designated C_{theor}. All of the C_{exp} are smaller than expected. A similar effect can be found in the data for the corresponding $R\mathrm{CrO}_3$ compounds (*3*) but it is much more pronounced here. For one case, ErTiO_3, the difference is quite large. A possible explanation for these discrepancies might lie in the combined effects of crystal-field-induced anisotropy and preferred orientation in the polycrystalline samples. It is well known that the interaction between the crystal field and the orbital moment of the rare earth ions can give rise to giant magnetocrystalline anisotropies and evidence for this effect will be presented later relevant to this series of compounds. Our samples consist of dense pellets pressed from coarse powders and in this form individual particles will be fixed relative to the magnetic field. We have observed that small crystals of the $R\mathrm{TiO}_3$ phases often show a plate-like habit. We are attempting to prepare single crystals of some of these compounds in order to investigate further the possibility of paramagnetic anisotropy.

Given the problem just outlined and the well-known deficiencies of the molecular field model it is not clear how much quantitative significance to attach to the molecular field coefficients, $\gamma_{\mathrm{Ti-Ti}}$, $\gamma_{R-\mathrm{Ti}}$, and γ_{R-R}. Nonetheless, conclusions can be drawn. $\gamma_{\mathrm{Ti-Ti}}$ is positive (ferromagnetic) and is generally larger by an order of magnitude than γ_{R-R}. This is reasonable as the critical temperatures, T_c, for the $R\mathrm{TiO}_3$ phases are an order of magnitude greater than those for

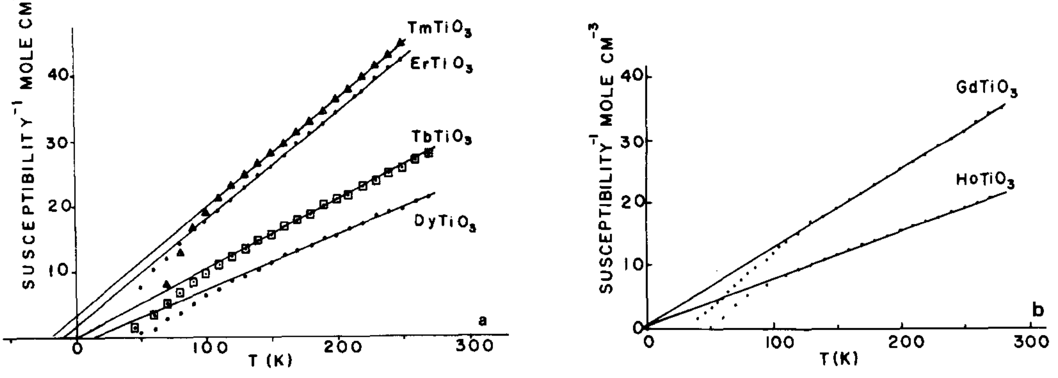

FIG. 2. (a) Inverse susceptibility as a function of temperature for *R* = Tb, Dy, Er, and Tm. (b) Inverse susceptibility as a function of temperature for *R* = Gd and Ho.

TABLE III

CURVE-FITTING PARAMETERS[a] DERIVED FROM HIGH-TEMPERATURE SUSCEPTIBILITIES AND ORDERING TEMPERATURES FROM LOW-FIELD MAGNETIZATION DATA FOR VARIOUS RTiO$_3$

R	T_c (K±2 K)	C_{exp}	$C_{\text{theor.}}$	θ (K)	ξ	θ' (K)	$\gamma_{R\text{-Ti}}$	$\gamma_{\text{Ti-Ti}}$	$\gamma_{R\text{-}R}$
Gd	34	8.12(3)	8.25	−4.7(9)	52(4)	41(1)	−5.6	9.5	−0.6
Tb	49	9.69(8)	12.19	−1(2)	40(4)	48(2)	−5.6	9.3	1.4
Dy	64	11.9(1)	14.54	16(1)	36(4)	52(2)	−3.0	9.1	2.2
Ho	56	13.40(4)	14.44	−5.4(7)	26(3)	52(1)	−4.3	6.3	0.76
Er	41	6.1(4)	11.85	−9(1)	18(2)	40(1)	−7.9	8.4	1.7
Tm	58	6.1(2)	7.52	−19.6(7)	55(7)	59(1)	−13.0	12.6	0.49
Lu[b]	30	—	—	—	—	—	—	—	—
Y[c]	29	0.36	0.37	33	—	—	—	9.4	—

[a] The four parameters were obtained from 40 to 50 data points in the range 300 K to ~T_c. The numbers in parentheses represent the standard error in the last significant figure. A more complete set of χ_m^{-1} vs T data than is shown in figs. 2a and b is available and may be obtained from the authors upon request.

[b] Reference (*6*) reports $T_c = 38$ K for "LuTiO$_3$."

[c] Reference (*6*).

the corresponding RAlO$_3$ compounds (*1*). Although there is apparent variation of $\gamma_{\text{Ti-Ti}}$ throughout the series, this may be an artifact of the fitting procedure, and it is interesting to note that the mean value and the sign of $\gamma_{\text{Ti-Ti}}$ for the entire series are very close to those for the ferromagnet, YTiO$_3$. The fact that T_c for LuTiO$_3$, also a ferromagnet (*6*), is nearly the same as that for YTiO$_3$ lends support to the thesis that $\gamma_{\text{Ti-Ti}}$ is ferromagnetic and invariant throughout this part of the RTiO$_3$ series. Such behavior is in sharp contrast to that exhibited by the RVO$_3$, RCrO$_3$, and RFeO$_3$ series in which the critical temperature and $\gamma_{M\text{-}M}$ decrease monotonically as the cell volume decreases from $R = $ Gd to $R = $ Lu (*14*). $\gamma_{R\text{-Ti}}$ is generally intermediate in magnitude between $\gamma_{\text{Ti-Ti}}$ and $\gamma_{R\text{-}R}$ and always antiferromagnetic. The wide variation in mâgnitude from compound may be a real effect.

Critical temperatures, T_c were determined from plots of σ^2 vs T data obtained at low fields, ca. 0.0045 T. These plots were reasonably linear near T_c and an example is shown as an inset of Fig. 3. The variation of T_c within the RTiO$_3$ series is not correlated with any obvious property of the crystal, such as cell volume, or any property of the R^{3+} ion, such as J, gJ, or S.

Magnetization measurements yield data of which those in Fig. 3 for ErTiO$_3$ are typical. From the shape of these curves there is no evidence that the R sublattice orders at a different temperature than the transition metal sublattice. Again this contrasts with

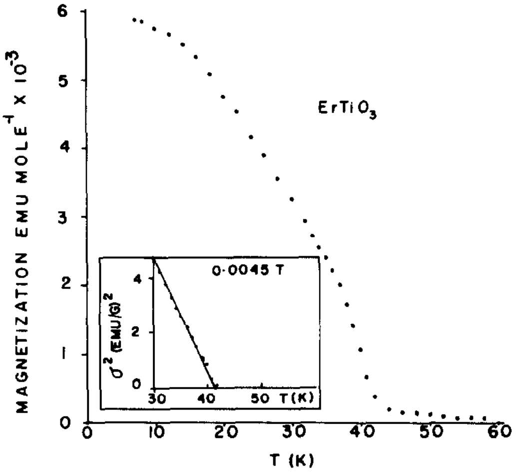

FIG. 3. Temperature dependence of the magnetization below the critical temperature for ErTiO$_3$. The applied field is 0.5 T. The inset shows the low-field (0.0045 T) σ^2 vs T plot used to estimate the critical temperature, T_c.

the behavior of $R\mathrm{VO}_3$, $R\mathrm{CrO}_3$, and $R\mathrm{FeO}_3$ as indicated in the introduction. The temperature dependence of the zero-field magnetization of certain of the $R\mathrm{TiO}_3$ compounds is currently under investigation by neutron diffraction techniques.

Isothermal magnetization versus applied field behavior is shown in figs. 4 and 5. The data for GdTiO_3 are quite different from those of the other members of the series in that there is a sharp rise at low fields reaching a value in excess of 5 μ_B at 1.5 T. Measurement to 6.0 T, not shown, indicate apparent saturation with a value of 6.0 μ_B. This is near the value expected for a colinear ferrimagnetic coupling between Gd^{3+} ($4f^7$) and Ti^{3+} ($3d^1$). Magnetization curves for the remaining members of the series show a pronounced "S" shape at low fields and never approach a value near that expected for a colinear structure even at fields up to 6.0 T (Fig. 5). Behavior of this sort might result from complex magnetic structures, the effects of magnetocrystalline anisotropy, or some combination. The fact that it occurs only for those R^{3+} species with large orbital moments suggests that mangetocrystalline anisotropy plays an important role. Neutron diffraction studies of the magnetic structures of some of these compounds are under way.

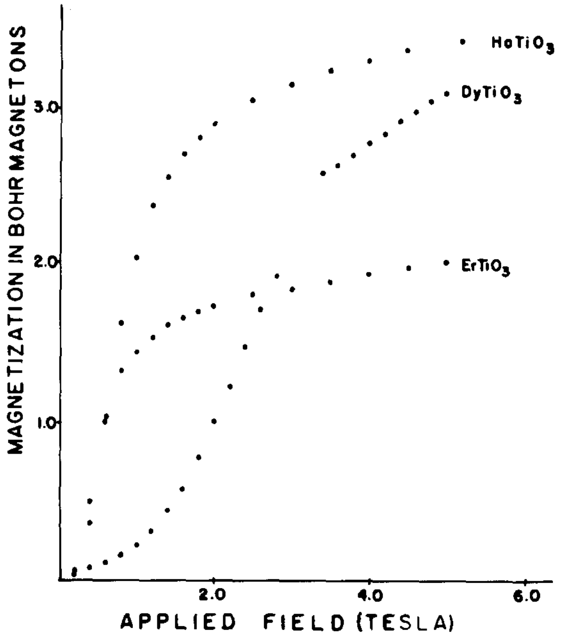

FIG. 5. Isothermal (4.2 K) magnetization versus applied field for various $R\mathrm{TiO}_3$ in the field range 0 → 6.0 T.

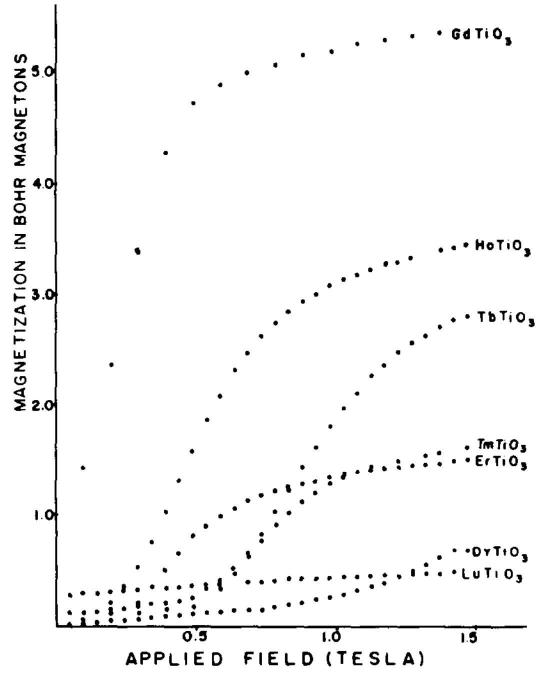

FIG. 4. Isothermal (4.2 K) magnetization versus applied field for various $R\mathrm{TiO}_3$ in the field range 0 → 1.5 T.

Summary and Conclusions

The compounds $R\mathrm{TiO}_3$ where $R = \mathrm{Gd}$, Tb, Dy, Ho, Er, and Tm are found to be ferrimagnets. Analysis of the exchange interactions on a molecular field model shows that the Ti–Ti interaction is ferromagnetic and the strongest coupling in the system. The R–Ti interaction is always antiferromagnetic and, while smaller than the Ti–Ti coupling, is of the same order of magnitude. This situation is quite unlike that for the related $RM\mathrm{O}_3$ compounds ($M = \mathrm{V}$, Cr, Mn, Fe) where the strong antiferromagnetic M–M interaction causes the R–M interaction to nearly vanish by symmetry.

Critical temperatures for the RTiO$_3$ series vary in an unpredictable manner with R. Anomalies in the low-temperature magnetization data suggest the importance of magnetocrystalline anisotropy combined with noncolinear magnetic structures.

Acknowledgments

We thank Dr. C. V. Stager for use of equipment and helpful discussions, and Mr. J. P. Goral for the GdTiO$_3$ data. The technical assistance of Mr. A. Quagglia and Mr. J. D. Garrett is acknowledged. Mr. H. F. Gibbs performed the neutron activation analysis. C.W.T. holds an Ontario Graduate Scholarship and the NSERC of Canada has supported this work with a research grant.

References

1. J. B. Goodenough and J. M. Longo, "Crystallographic and Magnetic Properties of Perovskite and Perovskite-Related Compounds," Landolt-Bornstein Tabellen Neve Serie III/4a, p. 126, Springer-Verlag, Berlin/New York (1970).
2. R. L. White, *J. Appl. Phys.* **40**, 1061 (1969).
3. E. F. Bertaut, J. Mareschal, G. de Vries, R. Aléonard, R. Pautlenet, J. P. Rebouillat, and V. Zarubicka, *IEEE Trans. Magn.* **MAG-2**, 453 (1966).
4. M. A. Gilleo, *J. Chem. Phys.* **24**, 1239 (1956).
5. R. M. Bozorth, H. J. Williams, and D. E. Walsh, *Phys. Rev.* **103**, 572 (1956).
6. D. C. Johnston, Ph. D. thesis, University of San Diego (1975).
7. P. Ganguly, Om. Parkash, and C. N. R. Rao, **36**, 669 (1976).
8. C. W. Turner, D. A. MacLean, and J. E. Greedan, "The Rare Earths in Science and Technology, 1978" (G. J. McCarthy and J. J. Rhyne, Eds.), p. 201, Plenum, New York (1978).
9. J. E. Greedan and D. A. MacLean, *Inst. Phys. Conf. Ser. No. 37*, 249 (1978).
10. G. V. Bazuev, V. A. Perelyaev, and G. R. Shveikin, *Inorg. Mater.* **10**, 915 (1974).
11. D. A. MacLean, H.-N. Ng, and J. E. Greedan, *J. Solid State Chem.* **30**, 35 (1979).
12. R. D. Shannon, *Acta Crystallogr. Sect. A* **32**, 751 (1976).
13. G. J. McCarthy, W. B. White, and R. Roy, *Mater. Res. Bull.* **4**, 251 (1969).
14. J. S. Smart, "Effective Field Theories of Magnetism," p. 114, Saunders, Philadelphia (1966).
15. M. Eibschutz, S. Shtrikman, and D. Treves, *Phys. Rev.* **156**, 562 (1967).